

# Exploring Thiol-Yne Based Monomers as Low Cytotoxic Building Blocks for Radical Photopolymerization

Andreas Oesterreicher,<sup>1</sup> Santhosh Ayalur-Karunakaran,<sup>2</sup> Andreas Moser,<sup>3</sup>  
Florian H. Mostegel,<sup>1</sup> Matthias Edler,<sup>1</sup> Petra Kaschnitz,<sup>4</sup> Gerald Pinter,<sup>3</sup> Gregor Trimmel,<sup>4</sup>  
Sandra Schlögl,<sup>2</sup> Thomas Griesser<sup>1</sup>

<sup>1</sup>Chair of Chemistry of Polymeric Materials & Christian Doppler Laboratory for Functional and Polymer Based Ink-Jet Inks, University of Leoben, Otto-Glöckel-Strasse 2, Leoben, 8700, Austria

<sup>2</sup>Polymer Competence Center Leoben GmbH, Roseggerstrasse 12, Leoben, 8700, Austria

<sup>3</sup>Chair of Material Science and Testing of Polymers, University of Leoben, Otto-Glöckel-Strasse 2, Leoben, 8700, Austria

<sup>4</sup>Institute for Chemistry and Technology of Materials (ICTM), NAWI Graz, University of Technology, Stremayrgasse 9, Graz, 8010, Austria

Correspondence to: T. Griesser (E-mail: thomas.griesser@unileoben.ac.at)

Received 28 April 2016; accepted 18 July 2016; published online 00 Month 2016

DOI: 10.1002/pola.28239

**ABSTRACT:** The last decade has seen a remarkable interest in the development of biocompatible monomers for the realization of patient specific medical devices by means of UV-based additive manufacturing technologies. This contribution deals with the synthesis and investigation of novel thiol-yne based monomers with a focus on their biocompatibility and also the mechanical properties in their cured state. It could be successfully shown that propargyl and but-1-yne-4-yl ether derivatives have a significant lower cytotoxicity than the corresponding (meth)acrylates with similar backbones. Together with appropriate thiol monomers, these compounds show reactivities in the range of (meth)acrylates and almost quantitative triple

bond conversions. A particular highlight is the investigation of the network properties of photo cured alkynyl ether/thiol resins by means of low field solid state nuclear magnetic resonance spectroscopy. Additionally, dynamic mechanical analysis of those polymers revealed that monomers containing rigid backbones lead to moduli and glass transition temperatures ( $T_g$ 's), sufficiently high for the fabrication of medical devices by UV based additive manufacturing methods. © 2016 Wiley Periodicals, Inc. *J. Polym. Sci., Part A: Polym. Chem.* **2016**, *00*, 000–000

**KEYWORDS:** low cytotoxicity; photopolymers; thiol-yne

**INTRODUCTION** Recent years have seen an increasing interest in the development of biocompatible, UV curable monomers for medical applications.<sup>1</sup> This fact can mainly be explained by the rapid progress in UV-based additive manufacturing technologies (AMTs), such as stereolithography, digital light processing, or three-dimensional (3D) ink-jet printing, which enable fast, accurate, and individual fabrication of biocompatible structures.<sup>2</sup>

Currently, monomers based on (meth)acrylates are the state-of-the-art UV curable materials for protective and decorative coatings.<sup>3–5</sup> These building blocks are characterized by their excellent storage stability and fast curing rates. Moreover, the mechanical properties of the resulting polymers can easily be adjusted by the choice of different spacers in photopolymerizable oligomers and by using different types of low molecular mono-, di-, and multifunctional (meth)acrylates as

reactive diluents. One considerable drawback of this class of chemical compounds is their comparably high irritancy and even cytotoxicity in their uncured state.<sup>6,7</sup> This disadvantageous behavior can be mainly attributed to the reactivity of the acrylate double bond toward Michael addition reactions with amino- or thiol-groups of proteins or DNA.<sup>8</sup> This fact, together with the incomplete curing behavior of (meth)acrylates (double bond conversions in the range of 60%–90% can usually be obtained) prevents their usability for medical purposes, that is, for materials which remain in contact with or within the human body.

Recently, several alternative radical curable functionalities, such as vinylcarbonates, vinylesters, and vinylcarbamates have been introduced as interesting alternatives to (meth)acrylate based resins providing a significant lower cytotoxicity.<sup>1,2,9</sup> However, the need of expensive reagents for the synthesis of

Additional Supporting Information may be found in the online version of this article.

© 2016 Wiley Periodicals, Inc.

those monomers along with their comparably low homopolymerization rates may explain why such resins have not entered the market so far.<sup>1</sup> In particular, compounds bearing easily abstractable hydrogens as, for example, in oligo ethylene glycol units are far less reactive than the corresponding acrylates. Although the addition of multifunctional thiols, which also provide very low cytotoxicity, accelerates the curing rates of those monomers toward values of acrylates, the Young's modulus and the glass transition temperature are lowered significantly. This fact can be attributed to a decrease in the cross-link density and also to the flexibility of the commonly used thiol compounds, that is, mercapto propionic ester derivatives, and the formed thioether bonds.<sup>9</sup>

In general, the addition of thiols to ene-monomers results in reduced resin stability (shelf-life) due to occurring dark polymerization reactions.<sup>10</sup> Another mentionable drawback is the characteristic odor of thiol monomers. Due to the limited network properties, thiol-ene photopolymers do not fulfill the demands of medical applications, such as dental restoratives or hard tissue replacements.<sup>11</sup> This fundamental limitation of the thiol-ene step growth polymerization is explained by the fact that each ene functional group reacts only once with a thiol, whereas in chain growth polymerization, each ene group becomes part of a polymer chain leading to higher network densities. Numerous approaches have been undertaken to increase the mechanical properties of thiol-ene polymers by using rigid ene and thiol compounds or monomers which are capable to form hydrogen bonds.<sup>10,12–15</sup>

Another possibility to enhance the network properties is to increase the network density of such photopolymers. An elegant approach is to use multifunctional alkynes instead of ene monomers.<sup>16–19</sup> In this so called thiol-yne polymerization a yne functional group reacts with a thiol to form a vinylsulfide, which can subsequently react with another thiol. Outside of the dual reactivity that offers a significant increase in the cross-link density, all other characteristics of the thiol-yne photopolymerization follow the ideal click reaction paradigm of thiol-ene systems. The polymerization is highly efficient and relatively unaffected by oxygen, ensuring the formed network being nearly ideal in homogeneity.

Fairbanks et al. studied systematically the relative reactivities of a range of different yne monomers revealing high reaction rates for terminal alkynes and propargyl esters.<sup>20</sup> Only moderate polymerization rates were found for propargylethers and internal alkynes. Cyclooctyne, methylpropargylamine and ethyl propiolate do not show this bireactive character.

Very recently, Pretzel et al. investigated the cytotoxic potential of internal alkynes. It was found that besides the type of the polymerizable moiety, also the spacer group of photo-reactive building blocks exerts significant influence on the curing and cytotoxic behavior.<sup>2,21</sup> Moreover, the network properties of the cured monomers strongly depend on the type and flexibility of the spacer. For example, monomers containing rigid structures such as bisphenol A moieties,

which are known to offer high moduli and high  $T_g$ 's, lead to comparably low curing rates and double bond conversions.<sup>22</sup>

Taking those facts into account, in the present article, the curing and cytotoxic behavior of propargyl and but-1-yne-4-yl monomers containing butyl (C4) spacers, that is, butanediol dipropargyl ether (BuPE) and butanediol di-1-butynyl ether (BuBE), were investigated and compared with the corresponding (meth)acrylate based compounds butanediol dimethacrylate (BuMAc) and butanediol diacrylate (BuAc). The network properties (cross-link density, glass transition temperature, and storage modulus) of these thiol-yne polymers were studied by solid state nuclear magnetic resonance (NMR) and dynamic mechanical analysis (DMA) measurements. Additionally, a second class of alkynyl ether based monomers bearing rigid spacers was investigated considering reactivity and network properties after UV polymerization. This study reveals the versatility of those monomers for the individual and patient customized fabrication of medical devices by UV-based additive manufacturing methods.

## EXPERIMENTAL

### NMR Studies

<sup>1</sup>H-NMR and <sup>13</sup>C-NMR spectra were recorded on a Varian 400-NMR spectrometer operating at 399.66 and 100.5 MHz, respectively, and were reference to Si(CH<sub>3</sub>)<sub>4</sub>. For the acquisition of the <sup>1</sup>H-NMR spectra a relaxation delay of 10 s and a 45° pulse were used. The NMR spectra were referenced to solvent residual peaks according to values given in the literature.<sup>23</sup>

<sup>1</sup>H-NMR spectra for real-time experiments were recorded on a Varian INOVA 500 MHz spectrometer operating at 499.803 MHz and were referenced to Si(CH<sub>3</sub>)<sub>4</sub>. A relaxation delay of 1 s and 45° pulse were used for acquisition of the <sup>1</sup>H-NMR spectra. The measurements were performed at 37 °C.

Low field NMR measurements were recorded on a Bruker minispec mq20 NF series spectrometer equipped with a 0.47 T magnet (<sup>1</sup>H resonance frequency of 20 MHz) and a ratio probe. The 90°, 180° pulse lengths and the receiver dead time were 2.8, 5.7, and 9 μs, respectively. The sample was cut into stripes, which were vertically stacked into the sample tube to fill a cylindrical volume of 8 mm diameter and 8 mm height. Measurements were carried out at 100 °C after an equilibration time of about 45 min. The sample was heated by dry air and the temperature regulated with a BVT3000 variable temperature controller.

DQ NMR measurements were carried out with the so-called 5-pulse segment<sup>24</sup> and the modified Baum-pines sequence. Further details of the measurement principle are given in the Supporting Information and were reviewed elsewhere.<sup>25</sup>

### Real-Time FT-IR Measurements

Kinetic real-time FT-IR measurements were conducted on a VERTEX 70 (Bruker, Billerica) in reflection mode with the unit A513. About 1 μL of the resin of investigation was

placed in between two CaF<sub>2</sub> windows (8 mm diameter, 1 mm thickness) and illuminated with an Omnicure s1000 (Lumen Dynamics, Mississauga) with 9 cm gap between the sample and light guide ( $P = 22 \text{ mW/cm}^2$  at the sample surface). For real-time FT-IR measurements the corresponding monomers were mixed with 5 wt % of the photoinitiator blend, diphenyl(2,4,6-trimethylbenzoyl)phosphine oxide/2-hydroxy-2-methylpropiophenone and a stoichiometric amount of trimethylolpropane tris(3-mercaptopropionate) (TMPMP). The corresponding (meth)acrylates were prepared without any thiol component. For thermal post-curing the sample was placed on a 100 °C heated plate and illuminated stepwise with the same intensity as described above.

### Photo-DSC

The photo-DSC experiments were performed on a NETZSCH photo-DSC 204 F1 Phoenix. All measurements were conducted at 50 °C in aluminum crucibles under nitrogen atmosphere. Sample quantity was 8 mg of resin, which was prepared in the same way as being described for real-time FT-IR measurements [5 wt % of the photoinitiator blend, diphenyl(2,4,6-trimethylbenzoyl)phosphine oxide/2-hydroxy-2-methylpropiophenone and a stoichiometric amount of TMPMP]. The Omnicure s2000 was used as the light source at 1 W/cm<sup>2</sup> resulting in an intensity of 80 mW/cm<sup>2</sup> at the surface of the sample (range of wavelength was 250–445 nm). For the determination of the reaction enthalpy and  $t_{\text{max}}$ , the samples were illuminated twice for 10 min each with an idle time of 2 min in between. For the analysis, the second run was subtracted from the first one to obtain the reaction enthalpy curve.

### Sample Preparation

For the determination of the thermomechanical properties of derived photopolymers sample specimens with  $2 \times 5 \times 20$  mm rectangular dimensions, respectively, were fabricated in PTFE molds. The resin samples were photocured by a Lighthammer 6 (Fusion UV Systems) with a Hg bulb (4 passes each side, belt speed of 4 m/min, 40% light intensity,  $E = 4.7 \text{ J/cm}^2$ ). The resin contained the corresponding alkyne with a stoichiometric amount of silanetetrayltetrakis(propene-1-thiol) and 3 wt % of the photoinitiator Irgacure® TPO-L. The  $T_g$  was determined at the maximum of tan delta.

### Dynamic Mechanical Thermal Analysis (DMA)

The thermomechanical properties were measured in tension mode using a DMA/SDTA 861 (Mettler Toledo) with a heating rate of 2 K/min in the temperature range from –40 °C to 115 °C. The operating frequency was determined at 1 Hz. For comparison of the alkyne ether formulations, the storage modulus was evaluated at room temperature (37 °C) and the glass transition temperature was determined at the maximum of tan delta.

### Viscosity Measurements

The viscosities of the monomers were determined using an Anton Paar rheometer (MCR-102, Graz, Austria) in a cone-plate system setup with titanium cone (MK 22/60 mm, 0.58°) with an opening angle of 0.58° and a diameter of

60 mm at a shear rate of  $300 \text{ s}^{-1}$ . The viscosity was measured at 25 °C.

### Cytotoxicity

The cytotoxicity experiments were conducted at Cytox biologische Sicherheitsprüfungen (Bayreuth, Germany) according to ISO 10993-5:2009. For these tests mouse fibroblast cells (L929) were used. Cells were cultured for 24 h in Dulbecco's modified Eagle's medium (DMEM) with added antibiotics, supplemented with 10% fetal calf serum at 37 °C in an incubator with 5% CO<sub>2</sub>. Four different concentrations of the examined substance (dissolved in DMSO) were applied onto the cells and incubated for 48 h at 37 °C with 5% CO<sub>2</sub>. The final concentration of DMSO in all cavities in the cell culture medium was 1% (v/v). Triton X 100 was used as toxic positive control [final concentration 1% (v/v)] and the cell culture medium was used as non-toxic negative control. All experiments were conducted four times simultaneously. After the incubation the L929-cells were washed with phosphate buffered saline (PBS), and after an alkaline lysis step the protein concentration was determined via the Bradford method. Graphical illustrations of the protein content in dependence of the monomer concentration can be found in the Supporting Information.

### Materials

2-Hydroxyethyl acrylate (Sigma Aldrich, 96%), 2-hydroxyethyl methacrylate (Sigma Aldrich, 99%), ethanolamine hydrochloride (Sigma Aldrich, 99%), 2-(2-methoxyethoxy)ethanethiol (97%), 1,4-dibromobutane (Sigma Aldrich, 99%), 2-propyn-1-ol (Sigma Aldrich, 99%), 3-butyn-1-ol (Sigma Aldrich, 97%), sodium hydride (Sigma Aldrich, 60% dispersion), tetrabutylammonium iodide (Sigma Aldrich, 98%), bisphenol A (Sigma Aldrich, 99%), ethylene carbonate (Sigma Aldrich, 99%), 3-bromo-1-propyne (Sigma Aldrich, 80 wt % in toluene), tetrachlorosilane (Sigma Aldrich, 99%), magnesium (Sigma Aldrich, 99.9%), 3-chloro-1-propene (Sigma Aldrich, 99%), 2,2'-azobis(2-methylpropanionitrile) (Fluka), thioacetic acid (Sigma Aldrich, 96%), ethyl(2,4,6-trimethylbenzoyl)phenylphosphinate (Irgacure® TPO-L, BASF), diphenyl(2,4,6-trimethylbenzoyl)phosphine oxide/2-hydroxy-2-methylpropiophenone, blend (Sigma Aldrich), pentaerythritol tetra(3-mercaptopropionate) (PETMP) (Sigma Aldrich, 99%), and trimethylolpropane tri(3-mercaptopropionate) (TMPMP) (Bruno Bock Chemische Fabrik GmbH & Co. KG) were used as received. 1,4-Butanediol diacrylate (abcr GmbH) and 1,4-butanediol dimethacrylate (abcr GmbH, 90%) have been purified by flash chromatography prior usage. Tetra(3-mercaptopropyl)silane (TMPS) was synthesized according to literature.<sup>26</sup>

### Synthesis

#### 1,4-Butanediol dipropargyl Ether (BuPE)

In a three-neck round-bottom flask 2.4 g (100.0 mmol, 2.7 eq) sodium hydride was washed two times with n-hexane and afterward suspended in 50 mL DMF. The mixture was purged with nitrogen and cooled down to –10 °C in an ethanol cooling bath. About 5.4 g (96.3 mmol, 2.6 eq) 2-propyn-

1-ol in 50 mL DMF was added dropwise over 30 min. The mixture was stirred for 2 h. Eight grams of (37.1 mmol) 1,4-dibromobutane in 50 mL DMF was added dropwise over a time span of 30 min. The reaction mixture was kept at 0 °C for further 3 h and quenched afterward with a saturated ammonium chloride solution. Afterward the mixture was extracted three times with diethyl ether and dried over Na<sub>2</sub>SO<sub>4</sub>. The combined organic extracts were concentrated under reduced pressure at elevated temperature to remove the excess of 2-propyn-1-ol and residual DMF. The crude product was further purified by flash column chromatography (ethyl acetate:cyclohexane 1:10) leading to 5.3 g (yield: 86%) of BuPE as a transparent and colorless liquid.

<sup>1</sup>H-NMR (δ, 400 MHz, 25 °C, CDCl<sub>3</sub>): 4.11 (d, 4H, CH<sub>2</sub>-C≡C); 3.52 (m, 4H, CH<sub>2</sub>-O); 2.52 (t, 2H, C≡CH); 1.66 (m, 4H, CH<sub>2</sub>-CH<sub>2</sub>-O) ppm.

<sup>13</sup>C-NMR: (δ, 100 MHz, 25 °C, CDCl<sub>3</sub>): 79.92 (s, 2C, -C≡C); 74.01 (s, 2C, -C≡C); 69.68 (s, 2C, C-O); 57.93 (s, 2C, C-C≡C); 26.08 (s, 2C, C-C-O) ppm.

#### 1,4-Butanediol dibut-3-yn-1-yl Ether (BuBE)

In a 500 mL three-neck round-bottom flask 3.00 g (125 mmol, 2.5 eq.) sodium hydride was washed two times with n-hexane and afterward suspended in 150 mL DMF. The mixture was purged with nitrogen and cooled down to -10 °C in an ethanol cooling bath. About 21.20 g 3-butyn-1-ol (300 mmol, 6 eq.) in 50 mL DMF was added dropwise over 30 min. The mixture was stirred for 2.5 h while the temperature was kept around 0 °C. About 1.30 g tetrabutylammonium iodide (3.5 mmol; 0.07 eq.) was added to the mixture before a solution of 10.80 g 1,4-dibromobutane (50 mmol) in 40 mL DMF was added dropwise over a time span of 30 min. The reaction mixture was kept at 0 °C for 4 h and quenched with a saturated solution ammonium chloride. Afterward the mixture was extracted three times with diethyl ether and dried over Na<sub>2</sub>SO<sub>4</sub>. The combined organic extracts were concentrated under reduced pressure at elevated temperature to remove the excess of 3-butyn-1-ol and residual DMF. The crude product was further purified by flash column chromatography (ethyl acetate:cyclohexane 1:20 → 1:10) leading to 3.3 g (yield: 34%) of BuBE as a transparent and colorless liquid.

<sup>1</sup>H-NMR (δ, 400 MHz, 25 °C, CDCl<sub>3</sub>): 3.55–3.48 (m, 8H, CH<sub>2</sub>-O-CH<sub>2</sub>); 2.45 (t, 4H, CH<sub>2</sub>-C≡C); 1.97 (t, 2H, C≡C-H); 1.65 (m, 4H, O-CH<sub>2</sub>-CH<sub>2</sub>) ppm.

<sup>13</sup>C-NMR: (δ, 100 MHz, 25 °C, CDCl<sub>3</sub>): 81.4 (s, 2C, -C≡C); 70.7 (s, 2C, O-C); 69.2 (s, 2C, -C≡C); 68.7 (s, 2C, C-C≡C); 26.2 (s, 2C, C-C-C); 19.8 (s, 2C, C-C≡C) ppm.

#### 2,2-Bis[4-(2-hydroxy)ethoxyphenyl]propane (BisAE)

The product was synthesized according to a modified literature procedure.<sup>27</sup> In a three-neck round-bottom flask equipped with a reflux condenser 20 g (87.6 mmol) bisphenol A and 17.7 g (201.5 mmol, 2.3 eq.) ethylene carbonate were added to 24.2 g (175 mmol, 2 eq.) K<sub>2</sub>CO<sub>3</sub> in 300 mL

DMF and refluxed at 145 °C for 3 h. The reaction mixture was then poured into 1.5 L deionized water. The resulting white precipitate was filtered and washed with water, with methanol and afterward with a small amount of cold THF. The remaining white powder was dried under vacuum at 70 °C to yield 18.0 g (65%) of BisAE.

<sup>1</sup>H-NMR (δ, 400 MHz, 25 °C, CDCl<sub>3</sub>): 7.15–7.13 (d, 4H, Ar-H); 6.83–6.81 (d, 4H, Ar-H); 4.07 (t, 4H, -CH<sub>2</sub>-O-); 3.95 (m, 4H, -CH<sub>2</sub>-OH); 1.64 (s, 6H, -CH<sub>3</sub>) ppm.

<sup>13</sup>C-NMR: (δ, 100 MHz, 25 °C, CDCl<sub>3</sub>): 156.42 (2C, Ar-C-O), 143.57 (2C, Ar-C), 127.78 (4C, Ar-C), 113.92 (4C, Ar-C), 69.09 (2C, O-C), 61.53 (2C, C-OH), 41.72 (1C, C-CH<sub>3</sub>), 31.02 (2C, CH<sub>3</sub>); ppm

#### 2,2-Bis[4-(2-(prop-2-yn-1-yloxy)ethoxyphenyl]propane (BisAEPE)

In a 250 mL three-neck round-bottom flask 0.9 g (37.9 mmol, 2.4 eq.) sodium hydride was washed with n-hexane and afterward suspended in 30 mL DMF. The mixture was purged with nitrogen and cooled down to -10 °C in an ethanol cooling bath. Five grams (15.8 mmol) of BisAE were dissolved in 30 mL DMF and added dropwise over 30 min. The mixture was stirred for 1 h while the temperature was kept around 0 °C. A solution of 4.7 g (39.5 mmol, 2.5 eq.) 3-bromo-1-propyne in 30 mL DMF was added dropwise over a time span of 30 min. The reaction mixture was stirred for 2 h while the mixture was allowed to reach room temperature. It was then quenched with a saturated solution of ammonium chloride, extracted with diethyl ether and dried over Na<sub>2</sub>SO<sub>4</sub>. The combined organic extracts were concentrated under reduced pressure to receive the crude product, which was further purified by flash column chromatography (ethyl acetate:cyclohexane 1:3) to yield 5.4 g (87%) of BisAEPE as a transparent, yellowish liquid.

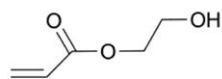
<sup>1</sup>H-NMR (δ, 400 MHz, 25 °C, CDCl<sub>3</sub>): 7.13–7.11 (d, 4H, Ar-H); 6.83–6.81 (d, 4H, Ar-H); 4.27 (d, 4H, CH<sub>2</sub>-C≡C); 4.13 (t, 4H, CH<sub>2</sub>-O-Ar); 3.89 (t, 4H, CH<sub>2</sub>-O); 2.45 (t, 2H, C≡C-H); 1.63 (s, 6H, CH<sub>3</sub>) ppm.

<sup>13</sup>C-NMR: (δ, 100 MHz, 25 °C, CDCl<sub>3</sub>): 156.47 (s, 2C, Ar-C-O); 143.41 (s, 2C, Ar-C); 127.69 (s, 4C, Ar-C); 113.94 (s, 4C, Ar-C); 79.49 (s, 2C, -C≡C); 74.69 (s, 2C, -C≡C); 68.26 (s, 2C, O-C); 67.11 (s, 2C, Ar-O-C); 58.53 (s, 2C, C-C≡C); 41.68 (s, 1C, Cq.); 31.03 (s, 2C, CH<sub>3</sub>) ppm.

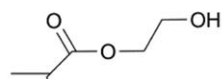
#### 2,2-Bis[4-(prop-2-yn-1-yloxy)phenyl]propane (BisAPE)

In a 250 mL three-neck round-bottom flask 1.3 g (52.6 mmol, 2.4 eq.) sodium hydride was washed with n-hexane and afterward suspended in 50 mL DMF. The mixture was purged with nitrogen and cooled down to -10 °C in an ethanol cooling bath. Five grams (21.9 mmol) of bisphenol A was dissolved in 50 mL DMF and added dropwise over 30 min. The mixture was stirred for 1 h while the temperature was kept around 0 °C. A solution of 6.8 g (57.2 mmol, 2.6 eq.) 3-bromo-1-propyne in 30 mL DMF was added dropwise over a time span of 30 min. The reaction mixture was stirred for

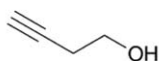
### Michael acceptors



HEA

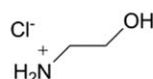


HEMA

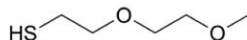


BuOH

### Michael donors



ETAHC



MTE

**SCHEME 1** Water soluble model compounds [HEA, 2-hydroxyethyl acrylate; HEMA, 2-hydroxymethyl acrylate; BuOH, 3-butyn-1-ol; ETAHC, ethanolamine hydrochloride; MTE, 2-(2-methoxyethoxy)ethanethiol] used for the evaluation of the reactivity of unsaturated functional groups.

2 h while the mixture was allowed to reach room temperature. It was then quenched with a saturated solution of ammonium chloride, extracted with diethyl ether and dried over  $\text{Na}_2\text{SO}_4$ . The combined organic extracts were concentrated under reduced pressure to receive the crude product, which was further purified by flash column chromatography (ethyl acetate:cyclohexane 1:5) to yield 6.1 g (92%) of BisAPE as a transparent and yellow liquid.

$^1\text{H-NMR}$  ( $\delta$ , 400 MHz, 25 °C,  $\text{CDCl}_3$ ): 7.17–7.15 (d, 4H, Ar–H); 6.89–6.87 (d, 4H, Ar–H); 4.67 (d, 4H, C=C–H); 2.52 (t, 2H, C=C–H); 1.64 (s, 6H,  $\text{CH}_3$ ) ppm.

$^{13}\text{C-NMR}$ : ( $\delta$ , 100 MHz, 25 °C,  $\text{CDCl}_3$ ): 155.4 (s, 2C, Ar–C); 143.9 (s, 2C, Ar–C); 127.7 (s, 4C, Ar–C); 114.2 (s, 4C, Ar–C); 78.8 (s, 2C, C=C); 75.35 (s, 2C, C=C); 55.8 (s, 2C, O–C); 41.8 (s, 1C, Cq.); 30.9 (s, 2C,  $\text{CH}_3$ ) ppm.

## RESULTS AND DISCUSSION

### Reactivity of Monomer Model Compounds Under Physiological Conditions

The cytotoxicity of state-of-the-art building blocks can be attributed to their reactivity toward amino- or thiol-groups of proteins or DNA.<sup>8</sup> In general, the electron density of unsaturated compounds, that is, the Michael acceptor, strongly determines the reactivity with (hetero) Michael donors.<sup>28,29</sup> Both facts can explain the lower cytotoxicity of methacrylates compared with their acrylate counterparts due to the higher electron density induced by the additional methyl group. Moreover, it is well reported that terminal alkyne groups, without electron withdrawing moieties in

their neighborhood, are mostly inert in the thiol Michael reaction even under basic conditions.<sup>30</sup>

The reactivity of radically polymerizable moieties toward amino and mercapto groups under physiological conditions was studied by  $^1\text{H-NMR}$  spectroscopy using  $\text{D}_2\text{O}$  soluble model compounds (as shown in Scheme 1). Taking into Account the pH-Value (pH  $\sim$  7.4) and the puffer capacity of blood, as well as the comparably high  $\text{pK}_b$  value of primary amines, it can be assumed that the majority of protein or DNA related amino groups exist in their protonated state. Considering this fact and the lower nucleophilicity of protonated amines, ethanolamine hydrochloride was chosen as model compound in the following experiments. For the exclusion of radical mediated reactions (e.g., thiol-ene) 0.1 wt % of pyrogallol was added as radical scavenger in all samples. Figure 1 shows the double bond conversion (DBC) of the (meth)acrylate model compounds during storage determined by kinetic NMR measurements at body temperature (37 °C). As expected, the acrylate, that is, HEA, shows the highest reactivity toward both nucleophiles. While the reaction with the mercapto group proceeds quantitatively within several minutes, a conversion of 30% was reached with ETAHC after 30 h.

Detailed NMR spectra confirmed the formation of the thiol Michael adduct, whereas the reaction with ETAHC lead to several by-products. Presumably, the formed secondary amine undergoes a subsequent Michael addition; furthermore, hydrolytic cleavage reactions of present ester groups are conceivable.

In contrast, HEMA shows a significant lower reactivity in both cases. Although it also provides full conversion in the reaction with MTE after 19 h, no formation of the aza Michael adduct could be observed, which can be assigned to the higher electron density of the C=C double bond (vide

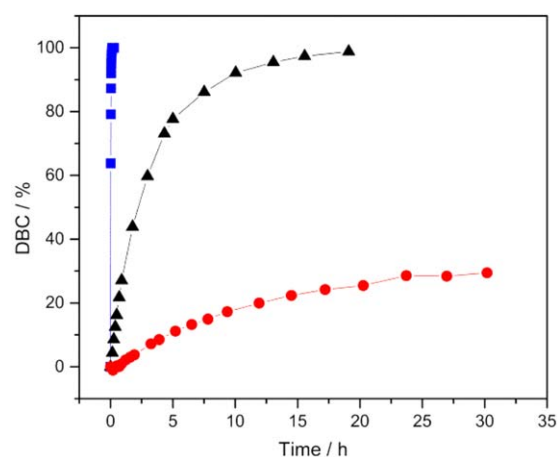
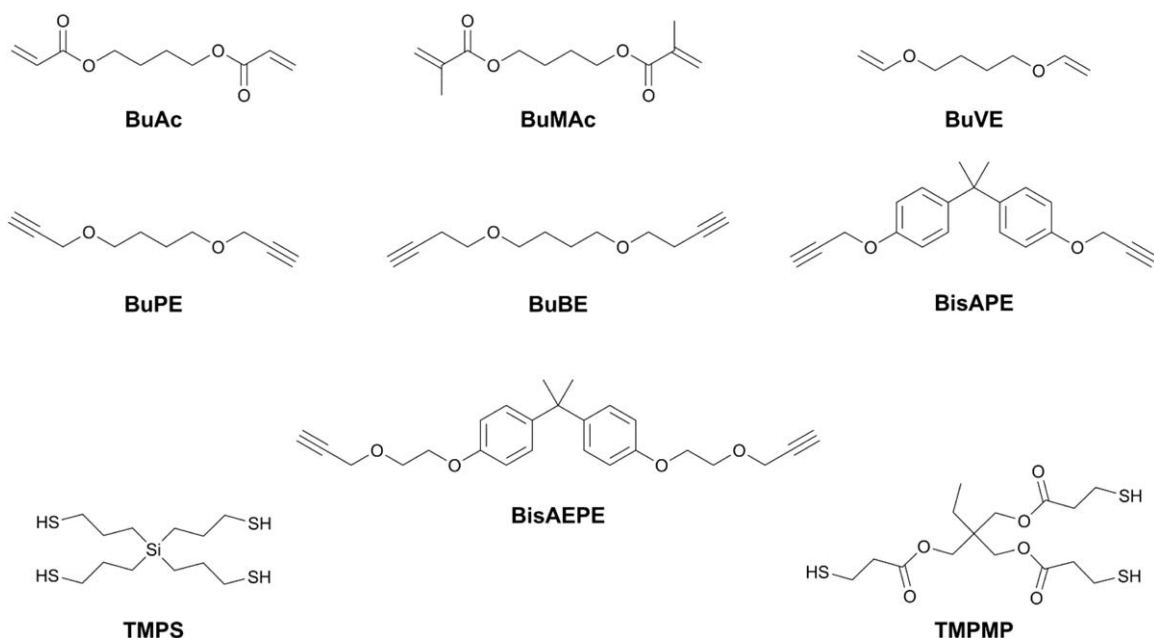


**FIGURE 1** Double bond conversion (DBC) of HEA/MTE (squares), HEMA/MTE (triangle), and HEA/ETAHC (circles) under simulated physiological conditions. [Color figure can be viewed in the online issue, which is available at [wileyonlinelibrary.com](http://wileyonlinelibrary.com).]



**Scheme 2** Structures of the investigated monomers.

supra). Importantly, under these conditions, the terminal alkyne group undergoes no reaction with any of the two Michael donors, neither with mercapto, nor with amino hydrochloride groups.

### Synthesis of Alkynyl Ether Monomers

An overview of the synthesized alkynyl ether based monomers is given in Scheme 2. A straightforward procedure for the preparation of those bifunctional ether derivatives, that is, BuPE, BuBE, BisAPE, and BisAEPE, represents the well described Williamson etherification reaction using hydroxyl- and bromo-functionalized starting compounds. For the synthesis of BisAEPE, the intermediate 2,2-bis[4-(2-hydroxy)ethoxyphenyl]propane was obtained by a reaction of bisphenol A with ethylene carbonate as described elsewhere.<sup>12</sup> In a first step, the hydroxyl terminated bifunctional spacers were converted with sodium hydride to the corresponding sodium alkoxylates, which were subsequently reacted with propargyl bromide to give BuPE, BisAPE, and BisAEPE in appropriate yields of 86%, 92%, and 87%. This reaction strategy, however, failed for the synthesis of the but-1-yne-4-yl ether derivatives leading to an isomerization of the triple bond and the formation of internal 2-yne. Alternatively, but-1-yne-4-yl ether monomers could be synthesized by the reaction of the sodium 3-butyne-1-olate with brominated bifunctional compounds as reported previously.<sup>31</sup> BuBE was obtained in moderate yields of 34% after purification by column chromatography. The synthesized monomers were characterized by <sup>1</sup>H- and <sup>13</sup>C-NMR spectroscopy. The obtained data are in good agreement with the proposed structures.

### Monomers with C4 Spacer

Besides the type of unsaturated polymerizable moiety and its reactivity toward the thiol and aza Michael reaction, also the group of photoreactive building blocks exerts significant influence on the cytotoxic behavior, which is a key requirement for UV curable resins for biomedical applications. For that reason the cytotoxic potential of the synthesized alkyne ether monomers with aliphatic C4 spacer, that is, BuPE and BuBE, was determined by *in-vitro* tests using mouse fibroblast cells (L929, ISO 10993-5:2009) and compared with the cytotoxicity of BuAc and BuMAc. Consequently, L929 cells were incubated in a defined media with increasing concentrations of the monomers for 48 h at 37 °C. The concentration at which the half of the cells remained alive compared with the negative control (cell culture medium, see Supporting Information) was assessed as cell viability (EC<sub>50</sub>). The (meth)acrylate based compounds (BuAc and BuMAc) exhibit a significant higher cytotoxicity than the alkynyl ethers BuPE and BuBE by at least a factor of 12 (as shown in Table 1). This finding is in good accordance with the observed inertia of terminal alkyne groups toward the thiol and aza Michael reaction. Thus, it could be demonstrated that alkynyl ether derivatives are a potential alternative to common (meth)acrylate based monomer systems.

Further important key factors for the fabrication of medical devices by photolithographic AMT techniques, are the rate and yield of photopolymerization, as both determine the amount of leachable monomers in the build device. Besides health considerations, residual monomers can also reduce the network properties, that is, mechanical properties and glass transition temperature, of the cured materials. The curing behavior of resins based on propargyl and but-1-yne-4-yl

**TABLE 1** Cell Viability of Investigated Monomers From Cytotoxicity Tests

Monomer	Viability (EC50)/mM
BuMAc	<0.16
BuAc	<0.16
BuPE	3
BuBE	2

monomers containing butyl (C4) spacers and the commercially available multifunctional thiol TMPMP were investigated by means of photo-DSC and FT-IR spectroscopy and compared with the corresponding (meth)acrylate based compounds BuMAc and BuAc. One important parameter, which can be obtained by photo-DSC, is the time to reach the maximum of polymerization enthalpy ( $t_{max}$ ) revealing information about the curing speed of the investigated system. Alternatively, real-time FT-IR spectroscopy provides detailed information on changes in the molecular structure of the monomers during the curing reaction, enabling the precise monitoring of the conversion of polymerizable groups with increasing illumination time.

Although, it has been reported that propargyl ether derivatives offer moderate rates of polymerization compared with aliphatic terminal alkynes and propargyl esters,<sup>20</sup> BuPE can easily compete with the methacrylate based monomer BuMAc which is reflected by the significant lower  $t_{max}$  as depicted in Table 2. Interestingly, the but-1-yne-4-yl ether derivative BuBE outperforms BuPE and BuMAc considerably and reacts only slightly slower than the structurally related aliphatic acrylate BuAc. The superiority of the but-1-yne-4-yl ether derivative might be explained by the additional CH<sub>2</sub> group between the alkyne and ether group reducing the influence of the ether moiety (+I-effect) on the electronic density of the yne triple bond. This hypothesis is supported by the outstanding reactivity of aliphatic terminal alkynes, which react significantly faster than propargyl ethers in the

thiol-yne reaction. However, a general prediction of reactivities based on the electronic density of polymerizable groups, as possible for the thiol-ene reaction, is problematic in case of the thiol-yne polymerization, which was shown by Fairbanks et al. at the example of propargyl acetate, methyl propargyl amine and ethyl propiolate.<sup>20</sup>

Figure 2 (above) shows the thiol and alkyne conversions for 2:1 stoichiometric reactions of BuPE/TMPMP and BuBE/TMPMP determined by real-time FT-IR spectroscopy, confirming the findings in the photo-DSC measurements and underlining the superiority of the but-1-yne-4-yl derivative in terms of reaction rate. It has to be mentioned that each alkyne and thiol monomer is consumed simultaneously and at the same extend, indicating the absence of side reactions such as the homopolymerization of vinylsulfide intermediates or the formation of stable vinylsulfide compounds. Importantly, both alkyne based systems provide a significant higher conversion of polymerizable groups than the curing of the corresponding (meth)acrylates as revealed in Figure 2 (below). While the photopolymerization of BuAc and BuMAc lead to a double bond conversion of 79% and 74% after 2 min of illumination ( $P = 22 \text{ mW/cm}^2$ ), respectively, an almost quantitative consumption of alkyne and thiol groups were obtained for resins of BuPE/TMPMP (94%) and BuBE/TMPMP (99%).

One limitation of thiol based photopolymers can mainly be attributed to specific characteristics of the used multifunctional thiols. The predominantly applied and studied thiols are esters of mercapto propionates and thio glycolates, which can be explained by their facile synthesis from readily available precursors. However, the polarity of the ester group and its affinity to water favors water absorption which decreases the mechanical performance by lowering the modulus, glass transition temperature and strength, all factors that are detrimental for medical applications such as implants. One strategy, to overcome this limitation is to use ester-free silane based mercaptanes providing an appropriate curing behavior and good mechanical

**TABLE 2** Summary of Materials Properties for Alkyne Monomers and Their Photocured Alkyne/Thiol Networks Including Reference Samples (BuAc and BuMAc)

Monomer	Viscosity (25 °C)/ mPa*s	$t_{max}/s$	Conversion (2 min)/ %	$T_g/^\circ C$	$E'$ at 37 °C/MPa	FWHM/ $^\circ C$
BuVE	–	1.0 <sup>a</sup>	–	$-35 \pm 0^b$	$17 \pm 1^b$	$10 \pm 0^b$
BuMAc	4.7	6.7	74	$50 \pm 38$	$1,650 \pm 20$	–
BuAc	4.4	1.8	79	$80 \pm 6$	$1,420 \pm 30$	–
BuPE	4.7	5.2 <sup>a</sup>	94 <sup>a</sup>	$34 \pm 1^b$	$255 \pm 30^b$	$42 \pm 0^b$
BuBE	6.2	2.3 <sup>a</sup>	99 <sup>a</sup>	$36 \pm 0^b$	$230 \pm 5^b$	$34 \pm 1^b$
BisAEPE	949	6.2 <sup>a</sup>	65 <sup>b</sup> (98) <sup>b,c</sup>	$58 \pm 0^{b,c}$	$1,200 \pm 75^{b,c}$	$20 \pm 0^{b,c}$
BisAPE	596	8.1 <sup>a</sup>	62 <sup>b</sup> (92) <sup>b,c</sup>	$100 \pm 1^{b,c}$	$1,860 \pm 10^{b,c}$	$59 \pm 0^{b,c}$

<sup>a</sup> Corresponds to a formulation with a stoichiometric amount of TMPMP.

<sup>b</sup> Corresponds to a formulation with a stoichiometric amount of TMPS.  
<sup>c</sup> Measured after post-curing at 100 °C.

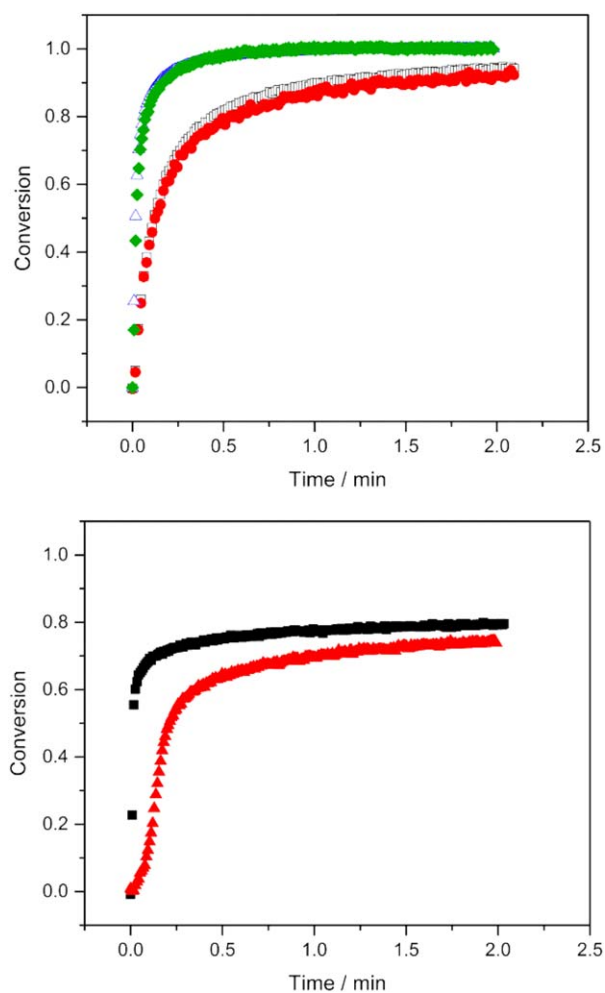


**FIGURE 2** Real-time FT-IR measurements: Conversion of alkyne and thiol moieties [above: BuBE (open triangle)/TMPMP (diamond), BuPE (open square)/TMPMP (circle)], and the (meth)acrylate groups [below: BuAc (square) and BuMAc (triangle)]. [Color figure can be viewed in the online issue, which is available at [wileyonlinelibrary.com](http://wileyonlinelibrary.com).]

properties in the cured state even after water storage as recently demonstrated.<sup>26,32</sup> Consequently, formulations containing the multifunctional thiol tetra(3-mercaptopropyl)silane (TMPS) instead of TMPMP were used for the characterization of the network properties. The synthesis of TMPS has previously been described in a patent dealing with novel biocompatible thiol-ene based materials for augmentation of hard tissues.<sup>33</sup> As shown recently, this thiol compound offers a comparable reactivity as mercapto propionic acid derivatives.<sup>26</sup>

It has to be mentioned that similar high conversions have been reported for thiol-ene polymerization reactions of vinyl-ethers, which are also known to provide good biocompatibility due to their electron rich double bond.<sup>34</sup> However, the comparably low cross-link densities of such thiol-ene networks lead to mechanical properties which are inferior compared with thiol-yne polymers.<sup>17</sup> Besides the mechanical

properties, the cross-link density, together with the structure of the polymer backbone, determines the glass transition temperature of the network, which has to be above body temperature for polymers intended for hard tissue engineering. There are only a few methods reported, which allow for the investigation of the network density of photopolymers. For several reasons some of them, for example, equilibrium swelling, can only be applied to slightly cross-linked polymers.<sup>35–37</sup> For very homogeneous networks, the cross-link density correlates with the glass transition temperature and the storage modulus in the rubbery state.<sup>17</sup>

An alternative method to study network characteristics is the DQ build-up NMR method<sup>38,39</sup> which gives quantitative access to network density as well as the fraction of non-network chains (in this case unreacted monomers, photoinitiator or its cleavage products which are not incorporated in the polymeric network). In simple terms, the residual dipolar couplings ( $D_{\text{res}}$ ) measured through this method are influenced by the orientational anisotropy of the chains which is in turn directly proportional to the cross-link density, that is, the molecular weight between the network points, and chain stiffness. The ability of this method to exclusively access  $D_{\text{res}}$ , allows a quantitative description of the network, assuming a physically appropriate model is used for analysis.

In this study, DQ NMR has been used to investigate and to compare the cross-link density of a vinyl ether based thiol-ene network with the highly cross-linked alkynyl ether networks. Consequently, butanediol divinylether (BuVE), BuPE, and BuBE (in combination with TMPS) were used as model compounds as these monomers provide a C4 backbone leading to a similar stiffness.

Considering that (a) the network chain length is near-homogenous and (b) any heterogeneity appears only due to the spin-system heterogeneity and/or the different mobility of the two component chains between network points, an analytical model assuming Gaussian distribution of residual dipolar couplings with an average value  $D_{\text{res}}$  and its standard deviation  $\sigma_{\text{res}}$  accounting for the aforementioned heterogeneity was used (see eq. 1).

Analytical fitting equation assuming Gaussian distribution

$$I_{\text{ndQ}}(\tau_{\text{DQ}}, D_{\text{res}}, \sigma_{\text{res}}) = 0.5 \left\{ 1 - \frac{\exp\left(-\frac{\frac{2}{5}D_{\text{res}}^2\tau_{\text{DQ}}^2}{1 + \frac{4}{5}\sigma_{\text{res}}^2\tau_{\text{DQ}}^2}\right)}{\sqrt{1 + \frac{4}{5}\sigma_{\text{res}}^2\tau_{\text{DQ}}^2}} \right\} \quad (1)$$

The  $D_{\text{res}}$  values (which relates to the cross-link density) and the fraction of non-network chains determined for samples BuBE/TMPS and BuPE/TMPS are given in Table 3. For comparison, measurements were also carried out on BuVE/TMPS and for consistency analyzed with the same model. It should be noted for the latter sample, however, that with  $\sigma_{\text{res}} \approx D_{\text{res}}$  (in other words a too high standard deviation), the limits of applicability of this fit becomes unrealistic. Therefore, the

**TABLE 3** Analysis of the Normalized DQ Curves Obtained for the Different Samples at 100 °C

Sample	$D_{res}/2\pi$ [kHz]	$\sigma_{res}/2\pi$ [kHz]	% Non-Network Chains
BuBE/TMPS	9.0	1.4	4.3
BuPE/TMPS	8.4	2.0	4.6
BuVE/TMPS (Gaussian distribution)	1.4	1.3	2.5

curve was also analyzed with a simple two-component Gaussian fit (see Supporting Information eq. S2).

The analysis (see Table 3) shows an increase in cross-link density by about the factor of six for samples BuBE/TMPS and BuPE/TMPS compared with sample BuVE/TMPS which is in good accordance with the findings of Bowman and co-workers for networks formed of bifunctionalynes and tetrafunctional thiols.<sup>17</sup> The fraction of non-network chains corresponds to the expected amount of unbound species (monomer, photoinitiator, cleavage products). Further details of the analysis and interpretation of the data for sample BuVE/TMPS are given in Supporting Information.

Moreover, the thermo-mechanical properties, that is, the glass transition temperature and the storage modulus in the rubbery state, of the thiol-yne networks are significantly higher than the BuVE network (shown in Fig. 3), which can be directly attributed to the higher cross-link density. The alkynyl ether/TMPS based polymers exhibit significant lower network properties than the corresponding (meth)acrylates BuAc and BuMAc (Table 2 and Fig. 3). While BuAc provides a  $T_g$  (~80 °C) well above the body temperature together with an appropriate storage modulus ( $E' = 1420$  MPa), the glass transition temperature of BuPE/TMPS (34 °C) and BuBE/TMPS (36 °C) is only in the range of body temperature explaining the comparably low moduli (BuBE:  $E' = 230$  MPa; BuPE:  $E' = 260$  MPa) at 37 °C. This fact can be attributed to the rather flexible (thio)ether linkage of the thiol-yne polymers.<sup>40</sup> Interestingly, there is only a slight difference, in the thermo-mechanical properties of BuBE and BuPE, despite two additional carbon atoms per molecule.

The full width at half-maxima (FWHM) of tan delta of the BuBE/TMPS and the BuPE/TMPS networks are approximately three times higher than the one of the BuVE/TMPS network. However, this transition is still narrow compared with chain growth networks, such as BuAc (see Fig. 3). However, materials that offer glass transition temperatures in the range or even below body temperature are not suitable for hard tissue engineering.

### Monomers Containing Rigid Spacers

One possibility to increase the network properties of photopolymers is to introduce rigid spacers such as biphenyl, isocyanurate,<sup>12</sup> bisphenol A,<sup>41</sup> bisphenol S,<sup>42</sup> etc., in the used

building blocks. This concept is commonly applied for high performance resins such as dental restoratives or automotive and aerospace resins; for example, 2,2-bis-[4-(2-hydroxy-3-methacryloyloxypropoxy)phenyl]-propane (Bis-GMA), is a widely applied monomer in dental practice. Although the stiff molecular structure of Bis-GMA is responsible for the excellent mechanical properties and low polymerization shrinkage, it also leads to an extremely high viscosity and to a comparably low degree of conversion.<sup>22</sup>

However, in these systems the gel point is reached very quickly, which significantly reduces the mobility of the unreacted functional monomers. An additional decrease in mobility can be observed when the  $T_g$  exceeds the polymerization reaction temperature. Both effects limit the final conversion of high viscous monomers containing rigid spacer.<sup>17</sup>

In principle, a similar behavior can also be observed for BisAPE/TMPS and BisAEPE/TMPS formulations as shown in Figure 4. While these bisphenol A based monomers exhibit curing rates in the range of BuPE, which seems to be typical

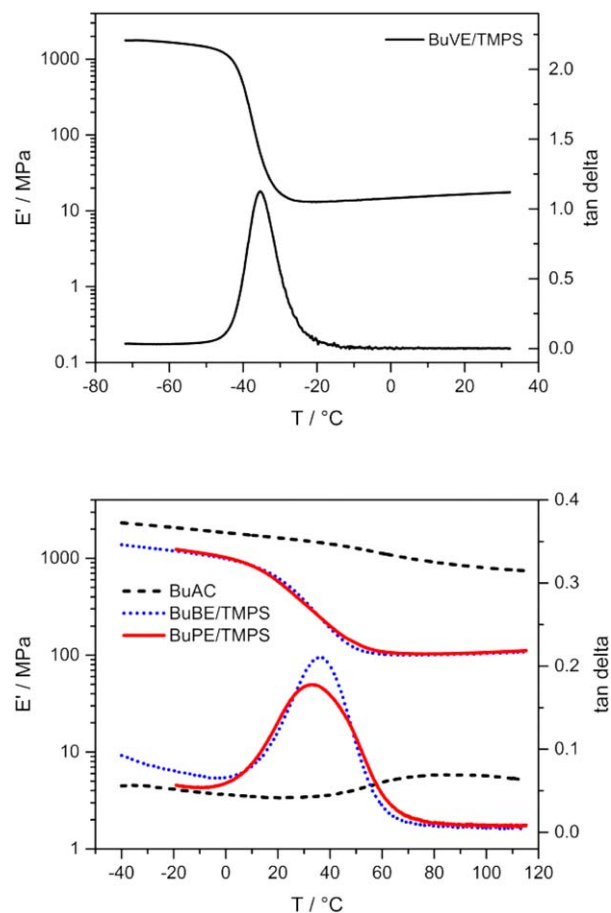


**FIGURE 3** Storage modulus and tan delta versus temperature for the stoichiometrically balanced polymerization of BuVE/TMPS (above), as well as BuAc (below: dashed), BuBE (below: dotted), and BuPE/TMPS (below: solid). [Color figure can be viewed in the online issue, which is available at [wileyonlinelibrary.com](http://wileyonlinelibrary.com).]

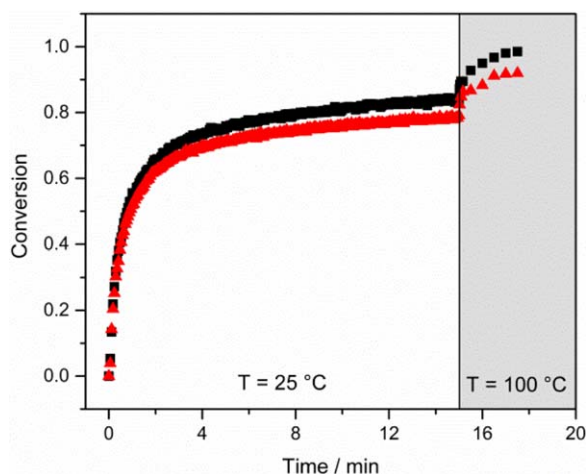


**FIGURE 4** Conversion of the alkyne monomers [BisAEPE (square), BisAPE (triangle)] in alkyne/TMPS formulations versus illumination time. [Color figure can be viewed in the online issue, which is available at [wileyonlinelibrary.com](http://wileyonlinelibrary.com).]

for propargyl ethers, the degree of conversion is comparably low for BisAPE/TMPS (62%) and BisAEPE/TMPS (65%).

However, it can be shown that a post curing of BisAPE and BisAEPE based resins above the  $T_g$  (in this case 100 °C were chosen) significantly increases the degree of conversion of both systems toward 92% (BisAPE) and 98% (BisAEPE), respectively, as demonstrated in Figure 4. This behavior is fully compatible with photolithographic AMT techniques, in which post curing of the printed structures is commonly performed, enabling the fabrication of biomedical devices with a low content of leachable monomeric residues.

As expected the networks formed of monomers with rigid spacers provide a significantly higher  $T_g$  as the corresponding C4 based polymers resulting in  $T_g$ 's which are well above the body temperature as depicted in Figure 5.

In particular, bisphenol A based monomers (with TMPS as thiol component) offer decent storage moduli (comparable to those of the C4 (meth)acrylic monomers) making these materials interesting for biocompatible AMT resins. Additionally, the comparably low FWHM of tan delta of BisAEPE/TMPS has to be highlighted, indicating a very homogeneous network and also providing almost constant mechanical properties over a long range up to 40 °C (=onset temperature of the glass transition; compare Fig. 5).

Another limiting factor of thiol based formulations is their poor shelf-life stability preventing a broad application in the UV curing and coating industry so far.<sup>10</sup> While formulations of BuVE/TMPMP (containing 0.5 wt % of pyrogallol and 2 wt % decylphosphonic acid as stabilizer) showed gelation after 4 h at 50 °C storage temperature, the corresponding thiol-yne resin, that is, BuBE/TMPMP (with the same stabilizer), increased in viscosity by only 22% after 1 week of storage under equal conditions. Presumably, the inertia of the alkyne triple bond toward Michael addition reactions

explains the superiority of the alkynyl ether/TMPMP formulation in this accelerated shelf-life tests, which represents another important advantage of the presented thiol-yne system.

## CONCLUSIONS

This contribution deals with the development of new biocompatible monomers based on the thiol-yne reaction for the fabrication of medical devices by UV-based additive manufacturing technologies. It could be successfully shown that propargyl and but-1-yne-4-yl ether derivatives offer a significant lower cytotoxicity than the corresponding (meth)acrylates with similar backbones. Together with appropriate thiol monomers, these compounds show reactivities in the range of acrylates (but-1-yne-4-yl ether) and methacrylates (propargyl ether), respectively, and almost quantitative triple bond conversions. Besides the reaction behavior, also the thermo-mechanical properties as well as the cross-link density of photo cured samples of alkynyl ether/thiol networks were investigated by DMA and solid state NMR and compared with those of BuVE/TMPS formulations. Although the BuPE/TMPS and BuBE/TMPS networks provide a six times higher cross-link density and thermo-mechanical properties, which are far above of the corresponding vinyl ether based network (BuVE/TMPS), these polymers show glass transition temperatures which are in the range of the body temperature. By using monomers that contain rigid bisphenol A spacers comparably high triple bond conversions after a post-curing step at elevated temperatures were obtained. The derived polymers show decent storage moduli and  $T_g$ 's which seems to be sufficiently high for the fabrication of medical devices.

Even though, the cytotoxicity of C4 alkynyl ethers is far lower than the one of the corresponding (meth)acrylates, the long term toxicity of such compounds, in particular of monomers containing bisphenol A moieties, has to be investigated in

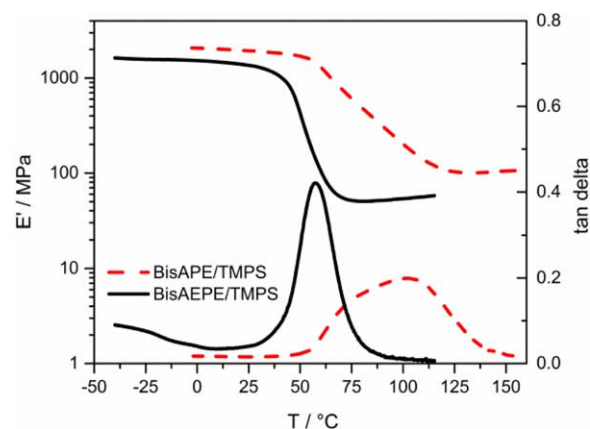


**FIGURE 5** Storage modulus and tan delta versus temperature for stoichiometrically balanced polymerization of BisAEPE/TMPS (solid) and BisAPE/TMPS (dashed). [Color figure can be viewed in the online issue, which is available at [wileyonlinelibrary.com](http://wileyonlinelibrary.com).]

further studies. However, the almost quantitative conversion of the investigated alkynyl ether/thiol resins significantly reduces the migration of potential harmful compounds to a level which cannot be reached by (meth)acrylate monomers.

This study reveals the versatility of this class of monomers paving the way toward the individual and patient specific fabrication of medical devices by UV-based additive manufacturing methods.

#### ACKNOWLEDGMENTS

Financial support by the Christian Doppler Research Association, the Austrian Federal Ministry of Science, Research and Economy (BMWFW), and Durst Phototechnik GmbH is gratefully acknowledged. Part of the research work of this paper was performed at the Polymer Competence Center Leoben GmbH (PCCL, Austria) within the framework of the COMET-program of the Federal Ministry for Transport, Innovation, and Technology and Federal Ministry for Economy, Family and Youth.

#### REFERENCES

- 1 B. Husar, R. Liska, *Chem. Soc. Rev.* **2012**, *41*, 2395.
- 2 C. Heller, M. Schwentenwein, G. Russmüller, T. Koch, D. Moser, C. Schopper, F. Varga, J. Stampfl, R. Liska, *J. Polym. Sci. A Polym. Chem.* **2011**, *49*, 650–661.
- 3 A. B. Scranton, C. N. Bowman, R. W. Peiffer, *Photopolymerization: Fundamentals and Applications*; American Chemical Society: Washington DC, **1997**, vol. 673.
- 4 N. S. Allen, *Photopolymerization and Photoimaging Science and Technology*, 1st ed.; Elsevier Applied Science: London, **1989**.
- 5 J. P. Fouassier, *Photoinitiation, Photopolymerization, and Photocuring: Fundamentals and Applications*; Hanser Publisher: New York, **1995**.
- 6 C. D. Calnan, *Contact Dermatitis* **1980**, *6*, 53–54.
- 7 L. S. Andrews, J. J. Clary, *J. Toxicol. Environ. Health.* **1986**, *19*, 149–164.
- 8 M. Friedman, J. F. Cavins, J. S. Wall, *J. Am. Chem. Soc.* **1965**, *87*, 3672–3682.
- 9 A. Mautner, X. Qin, G. Kapeller, G. Russmüller, T. Koch, J. Stampfl, R. Liska, *Macromol. Rapid Commun.* **2012**, *33*, 2046–2052.
- 10 C. E. Hoyle, T. Y. Lee, T. Roper, *J. Polym. Sci. A Polym. Chem.* **2004**, *42*, 5301–5338.
- 11 A. Lowe, C. Bowman, *Thiol-X Chemistries in Polymer and Materials Science*, RSC Publishing: Cambridge, **2013**.
- 12 S. Reinelt, M. Tabatabai, N. Moszner, U. K. Fischer, A. Utterodt, H. Ritter, *Macromol. Chem. Phys.* **2014**, *215*, 1415–1425.
- 13 J. A. Carioscia, J. W. Stansbury, C. N. Bowman, *Polymer* **2007**, *48*, 1526–1532.
- 14 Q. Li, H. Zhou, D. A. Wicks, C. E. Hoyle, *J. Polym. Sci. A Polym. Chem.* **2007**, *45*, 5103–5111.
- 15 S. Parker, R. Reit, H. Abitz, G. Ellson, K. Yang, B. Lund, W. E. Voit, *Macromol. Rapid Commun.* **2016**, *37*, 1027–1032.
- 16 A. B. Lowe, *Polymer* **2014**, *55*, 5517–5549.
- 17 B. D. Fairbanks, T. F. Scott, C. J. Kloxin, K. S. Anseth, C. N. Bowman, *Macromolecules* **2009**, *42*, 211–217.
- 18 J. W. Chan, J. Shin, C. E. Hoyle, C. N. Bowman, A. B. Lowe, *Macromolecules* **2010**, *43*, 4937–4942.
- 19 J. W. Chan, H. Zhou, C. E. Hoyle, A. B. Lowe, *Chem. Mater.* **2009**, *21*, 1579–1585.
- 20 B. D. Fairbanks, E. A. Sims, K. S. Anseth, C. N. Bowman, *Macromolecules* **2010**, *43*, 4113–4119.
- 21 D. Pretzel, B. Sandmann, M. Hartlieb, J. Vitz, S. Hölzer, N. Fritz, N. Moszner, U. S. Schubert, *J. Polym. Sci., Part a: Polym. Chem.* **2015**, *53*, 1843–1847.
- 22 F. Goncalves, Y. Kawano, C. Pfeifer, J. W. Stansbury, R. R. Braga, *Eur. J. Oral Sci.* **2009**, *117*, 442–446.
- 23 H. E. Gottlieb, V. Kotlyar, A. Nudelman, *J. Org. Chem.* **1997**, *62*, 7512–7515.
- 24 M. A. Voda, D. E. Demco, J. Perlo, R. A. Orza, B. Blümich, *J. Magn. Reson.* **2005**, *172*, 98–109.
- 25 K. Saalwächter, *Prog. Nucl. Magn. Reson. Spectrosc.* **2007**, *51*, 1–35.
- 26 M. Roth, A. Oesterreicher, F. H. Mostegel, A. Moser, G. Pinter, M. Edler, R. Piock, T. Griesser, *J. Polym. Sci. Part a: Polym. Chem.* **2016**, *54*, 418–424.
- 27 S. A. Caldarelli, S. El Fangour, S. Wein, C. van Tran Ba, C. Perigaud, A. Pellet, H. J. Vial, S. Peyrottes, *J. Med. Chem.* **2013**, *56*, 496–509.
- 28 E. D. Bergmann, D. Ginsburg, R. Pappo, *Org. React.* **1959**, *10*, 179–556.
- 29 D. P. Nair, M. Podgórski, S. Chatani, T. Gong, W. Xi, C. R. Fenoli, C. N. Bowman, *Chem. Mater.* **2014**, *26*, 724–744.
- 30 H. Peng, C. Wang, W. Xi, B. A. Kowalski, T. Gong, X. Xie, W. Wang, D. P. Nair, R. R. McLeod, C. N. Bowman, *Chem. Mater.* **2014**, *26*, 6819–6826.
- 31 I. N. Michaelides, B. Darses, D. J. Dixon, *Org. Lett.* **2011**, *13*, 664–667.
- 32 M. Podgórski, E. Becka, S. Chatani, M. Claudino, C. N. Bowman, *Polym. Chem.* **2015**, *6*, 2234–2240.
- 33 A. R. Molenberg, E. Zamparo, L. Rapillard, S. Cerritelli, WO 2011004255, *Compositions for Tissue Augmentation*, **2011**.
- 34 M. Sangermano, *Pure Appl. Chem.* **2012**, *84*, 2089–2101.
- 35 P. J. Flory, *Principles of Polymer Chemistry*; Cornell University Press: Ithaca, NY, **1953**.
- 36 P. J. Flory, J. Rehner, *J. Chem. Phys.* **1943**, *11*, 521.
- 37 P. J. Flory, *J. Chem. Phys.* **1950**, *18*, 108.
- 38 R. Graf, D. E. Demco, S. Hafner, H. W. Spiess, *Solid State Nucl. Magn. Reson.* **1998**, *12*, 139–152.
- 39 M. Schneider, L. Gasper, D. E. Demco, B. Blümich, *J. Chem. Phys.* **1999**, *111*, 402.
- 40 N. Moszner, W. Schöb, V. Rheinberger, *Polym. Bull.* **1996**, *37*, 289–295.
- 41 N. Moszner, U. Salz, *Macromol. Mater. Eng.* **2007**, *292*, 245–271.
- 42 S. Reinelt, M. Tabatabai, U. K. Fischer, N. Moszner, A. Utterodt, H. Ritter, *Beilstein J. Org.* **2014**, *10*, 1733–1740.